Bioorganic & Medicinal Chemistry 20 (2012) 3470–3479

Contents lists available at SciVerse ScienceDirect

Bioorganic & Medicinal Chemistry

journal homepage: www.elsevier.com/locate/bmc

Synthesis and binding properties of new selective ligands for the nucleobase opposite the AP site

Yukiko Abe [a], Osamu Nakagawa [a], Rie Yamaguchi [a], Shigeki Sasaki [a,b,*]

[a] Graduate School of Pharmaceutical Sciences, Kyushu University, 3-1-1 Maidashi, Higashi-ku, Fukuoka 812-8582, Japan
[b] Core Research for Evolution Science and Technology (CREST), Japan Science and Technology Agency, 4-1-8 Motomachi, Kawaguchi, Saitama 332-0012, Japan

ARTICLE INFO

Article history:
Received 19 March 2012
Revised 3 April 2012
Accepted 4 April 2012
Available online 10 April 2012

Keywords:
AP site
DNA
Binding ligand
Surface plasmon resonance
Isothermal titration calorimetry

ABSTRACT

DNA is continuously damaged by endogenous and exogenous factors such as oxidative stress or DNA alkylating agents. These damaged nucleobases are removed by DNA N-glycosylase and form apurinic/apyrimidinic sites (AP sites) as intermediates in the base excision repair (BER) pathway. AP sites are also representative DNA damages formed by spontaneous hydrolysis. The AP sites block DNA polymerase and a mismatch nucleobase is inserted opposite the AP sites by polymerization to cause acute toxicities and mutations. Thus, AP site specific compounds have attracted much attention for therapeutic and diagnostic purposes. In this study, we have developed nucleobase–polyamine conjugates as the AP site binding ligand by expecting that the nucleobase part would play a role in the specific recognition of the nucleobase opposite the AP site by the Watson–Crick base pair formation and that the polyamine part should contribute to the access of the ligand to the AP site by a non-specific interaction to the DNA phosphate backbone. The nucleobase conjugated with 3,3′-diaminodipropylamine (A-ligand, G-ligand, C-ligand, T-ligand and U-ligand) showed a specific stabilization of the duplex containing the AP site depending on the complementary combination with the nucleobase opposite the AP site; that is A-ligand to T, G-ligand to C, C-ligand to G, T- and U-ligand to A. The thermodynamic binding parameters clearly indicated that the specific stabilization is due to specific binding of the ligands to the complementary AP site. These results have suggested that the complementary base pairs of the Watson–Crick type are formed at the AP site.

1. Introduction

DNA is continuously damaged by either endogenous or exogenous agents such as reactive oxygen species, DNA alkylating agents, etc.[1,2] For example, the oxidation of guanosine at the 8-position produces 8-oxoguanosine which is an important marker of oxidative stress. The alkylation of guanosine at the N^7-position or adenosine at the N^3-position by alkylating agents produces 7-methylguanosine[3] or 3-methyladenosine,[4] respectively. These damaged nucleotides are removed by the base excision repair pathway to form the apurinic/apyrimidinic site (AP sites) as the intermediate.[5] AP sites per se are DNA damages and can spontaneously occur at a rate about 10,000 sites per day in human cells.[6] AP sites affect the local and global structures of DNA and it is known that unrepaired AP sites block DNA polymerase leading to acute toxicities[7] or preferentially incorporate deoxyadenosine opposite the AP site to induce mutations in the DNA polymerization.[8] The AP site stimulates topoisomerase II-mediated DNA cleavage to induce cell death.[9] Thus, the AP site-specific molecules would be useful for a better understanding of its biological impacts.[10] An attractive application of the AP site-specific molecules is to block the AP site repair in order to enhance the antitumor efficacy of the alkylating anticancer agents.[11,12] The AP site is in equilibrium between the hemiacetals, the hydrate form, and the aldehyde, which is targeted by the covalent bond with small molecular ligands though the Schiff base formation followed by reduction.[13] Non-covalent recognition of the AP site has also been investigated using non-natural nucleotides,[14] non-nucleoside probes,[15] nucleobase derivatives,[16] etc. The compounds that can recognize the remaining nucleobase opposite the AP sites would be useful to analyze the nature of the damage leading to the AP site. It can be also expected that the compound specific to the cytosine base opposite the AP site might potentiate the effect of the guanosine-alkylating agents. Despite a number of examples, it is difficult to rationally design molecular probes with selectivity to a nucleobase opposite the AP site. Lhomme's group developed adenine–acridine conjugates as DNA cleaving agents in which the adenine base was expected to locate in the AP site pocket and forms the complementary base pair with the thymine opposite the AP site. The strong binding of the acridine with the duplex DNA either by stacking or in the external binding mode was thought to bring the adenine base into the AP site pocket for the binding with the thymine base

* Corresponding author.
E-mail address: sasaki@phar.kyushu-u.ac.jp (S. Sasaki).

0968-0896/$ - see front matter © 2012 Elsevier Ltd. All rights reserved.
http://dx.doi.org/10.1016/j.bmc.2012.04.009

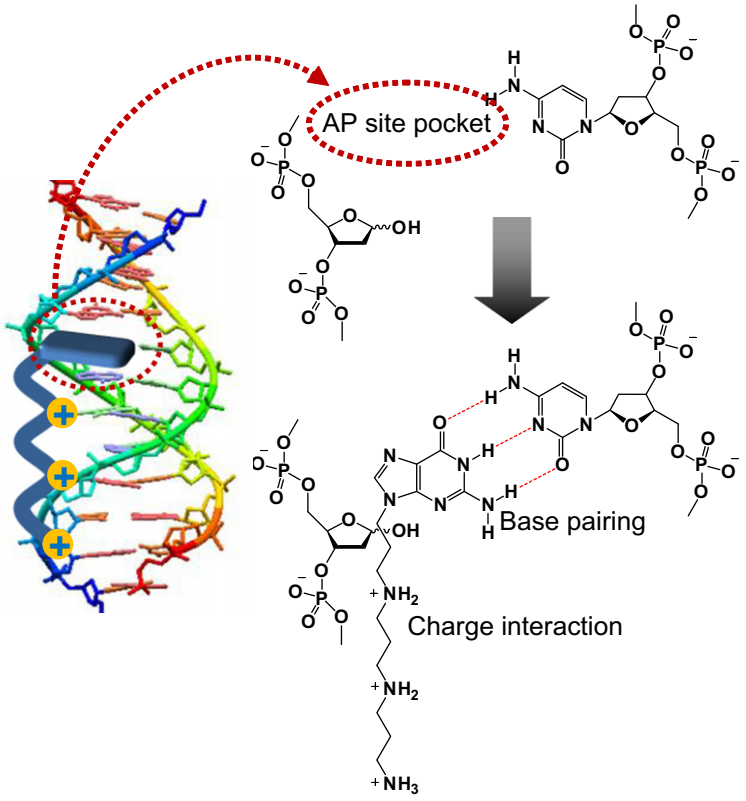

Figure 1. Design strategy for AP sites ligands with a selectivity to the opposing nucleobase.

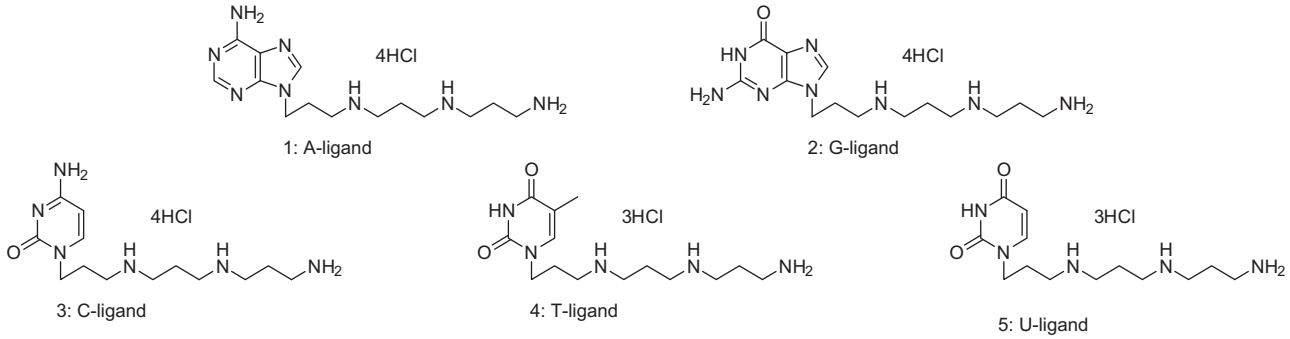

Figure 2. Nucleobase–polyamine conjugates.

opposite the AP site.[17] They also applied the AP site-binding ligand to enhance the in vivo toxicity of the alkylating agent (bischloroethylnitrosourea).[12] Encouraged by these studies, we hypothesized that the nucleobase might generally form Watson–Crick base pairs if the nucleobase is properly placed in the AP site pocket. In order to bring the nucleobase around the duplex DNA close the AP site, we relied on the weak electrostatic interaction of the polycation with the phosphate backbone. We now describe in detail the molecular design, synthesis and the binding properties with the duplex DNA containing the AP site.

2. Results and discussion

2.1. Design and synthesis of the nucleobase-3,3′-diaminodipropylamine conjugates

In our attempt to form A–T and G–C Watson–Crick base pairs in the AP site pocket, we designed nucleobase–polyamine conjugates (Fig. 1). The polycation unit was expected to promote access of the nucleobase to the duplex DNA by a non-specific, electrostatic interaction. When the nucleobase enters the AP site pocket, as the AP site pocket has a relatively hydrophobic nature, the complementary base pairing with the nucleobase opposite the AP site should produce the specific binding affinity of the ligand. Thus, the objective of this study is to confirm the binding selectivity of the nucleobase–polyamine conjugates in a predictable manner based on the Watson–Crick pairing. We employed 3,3′-diaminodipropylamine (norspermidine)[18] as the polyamine part in this study, because a weak DNA binding affinity of the polycation part was thought to be preferable in order to prove that the selectivity originated due to the nucleobase part. Biological polyamines, such as spermine, was not chosen because of the relatively higher affinity with some sequence preference.[19–21] Thus, five nucleobase conjugates with 3,3′-diaminodipropylamine were synthesized and subjected to measuring the binding properties (Fig. 2, A-ligand (**1**), G-ligand (**2**), C-ligand (**3**), T-ligand (**4**) and U-ligand (**5**)).

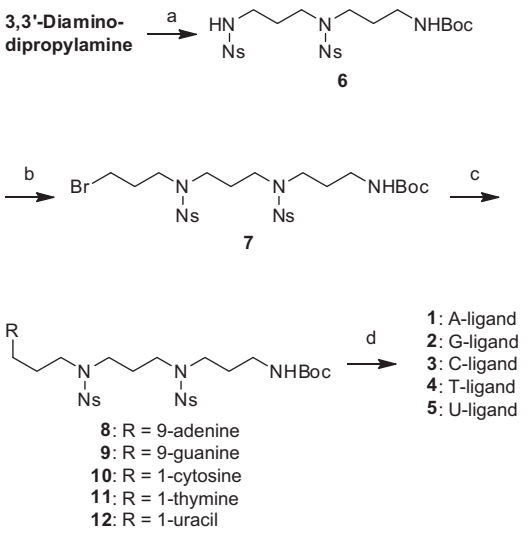

Scheme 1. The synthesis of the ligands (**1**–**5**). Reagents and conditions: (a) (i) $(Boc)_2O$, THF, 0 °C; (ii) NsCl, Et_3N, CH_2Cl_2, 0 °C; (b) 1,3-dibromopropane, K_2CO_3, DMF, rt; (c) (i) K_2CO_3, DMF, 60 °C, adenine for **1**; 2-amino-6-chloropurine for **2**, and then 0.5 M HCl/MeOH; 4-*N*-acetylcytosine for **3**; 3-*N*-benzoylthymine for **4**; 3-*N*-benzoyluracil for **5**, (d) (i) thiophenol, K_2CO_3, DMF, rt; (ii) 0.5 M HCl/MeOH, rt, or 10% aq HCl.

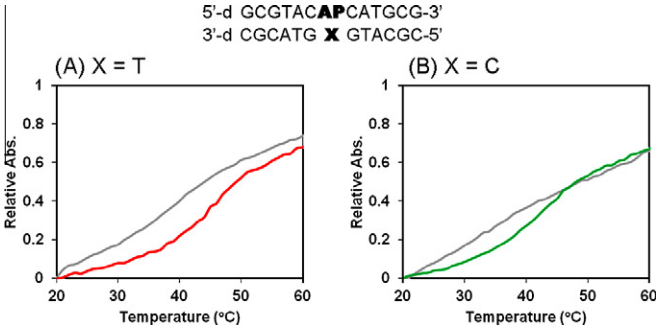

Figure 3. UV-melting curves in the absence (gray line) and presence of A-ligand (red line) or G-ligand (green line). (A) A-ligand and thymine opposite the AP site, (B) G-ligand and cytosine opposite the AP site. UV-melting curves were measured in 10 mM HEPES–NaOH buffer (pH 7.0), 100 mM NaCl at the scan rate of 1 °C at 260 nm in the absence and presence of the ligand. [duplex ODNs]: 4 μM, [ligands]: 20 μM. **AP** and **X** represent the tetrahydrofuran part and the nucleobase opposite the AP site, respectively.

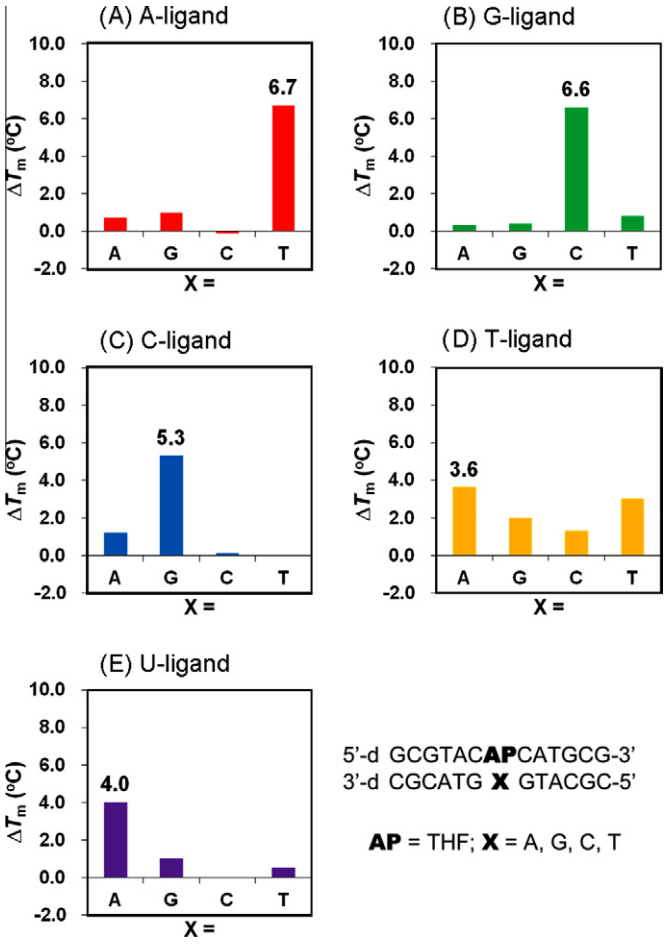

Figure 4. The selective stabilization effects of the ligand to the duplex ODN containing the AP site. [NaCl]: 100 mM for A-, G-ligands and [NaCl]: 50 mM for C-, T- and U-ligands. **AP** and **X** represent the tetrahydrofuran part and the nucleobase opposite the AP site, respectively.

The synthesis of the ligands is shown in Scheme 1. The terminal amino group of 3,3′-diaminodipropylamine was protected with the *tert*-butoxycarbonyl (*t*-Boc) group and the remaining amino groups were reacted with 2-nitrobenzenesulfonyl chloride (NsCl). The terminal nosylated amino group was reacted with 1,3-dibromopropane to form the triamine bromide **7** as the common intermediate. The nucleobase was alkylated with the bromide **7** to produce the corresponding nucleobase derivatives (**8**–**12**). Finally, all the protecting groups were removed to produce the nucleobase–polyamine conjugates (**1**–**5**). All ligands were purified as the hydrochloride salts.

2.2. Stabilization effects of ligands on duplex DNAs containing the AP site

The binding property of the ligand was evaluated by measuring the increase in the melting temperature (T_m) of the duplex DNA containing the AP site. The tetrahydrofuran ring was used as the stable AP site analog in the sequence of 5′-dGCG TAC **AP** CAT GCG-3′, where **AP** represents the THF ring. Duplexes were formed with the complementary sequence of 5′-dCGC ATG **X** GTA CGC-3′, where **X** represents the adenine, guanine, cytosine or thymine base opposite the AP site (**X** = A, G, C, T). Figure 3 illustrates the UV-melting curves obtained using the duplex (5′-dGCG TAC **AP** CAT GCG-3/5′-dCGC ATG **X** GTA CGC-3′) in the absence and presence of the A-ligand (Fig. 3A) or the G-ligand (Fig. 3B). The A-ligand selectively increased the T_m value of the duplex having X = T (ΔT_m = +6.7 °C), and the duplex incorporating X = C was selectively stabilized by the G-ligand (ΔT_m = +6.6 °C). The T_m value of other duplexes were not significantly changed (Fig. S1).

The increase in the T_m values are displayed in the bar graphs of Figure 4 and the data are shown in Table 1, clearly indicating the selective stabilization of the A-ligand for the opposing T and the G-ligand for opposing C (Fig. 4, A and B). The UV melting experiments using the C-, T- and U-ligands were performed in the buffer containing 50 mM NaCl to observe the clear effect of the ligand (UV-melting curves are shown in Fig. S2), and the increase in the T_m values are summarized in Figure 4 (C and D). Interestingly, the C-ligand showed a selective stabilization for G opposite the AP site (Fig. 4C, ΔT_m = +5.3 °C). In the case of the T-ligand, although the selective stabilization was observed for the opposing A, some stabilization was also observed for the opposing T and G (Fig. 4D, ΔT_m = +3.6 °C for A, +2.1 °C for G, and +3.0 °C for T). The formation of the G–T and T–T pairs might contribute to the weak stabilization. It should be noted that the U-ligand retained its selectivity to the opposing A, but lost the stabilization effect for the opposing

Table 1
Melting temperature of duplexes containing the AP site in the absence ($T_m(-)$) and presence ($T_m(+)$) of each ligand[a]

X =	Ligand									
	A-Ligand[b]		G-Ligand[b]		C-Ligand[c]		T-Ligand[c]		U-Ligand[c]	
	T_m (−)	T_m (+)	T_m (−)	T_m (+)	T_m (−)	T_m (+)	T_m (−)	T_m (+)	T_m (−)	T_m (+)
A	39.7	40.4 (+0.7)	40.1	40.4 (+0.3)	34.0	35.2 (+1.2)	35.6	39.2 (+3.6)	35.0	39.1 (+4.1)
G	39.8	40.8 (+1.0)	40.5	40.9 (+0.4)	35.2	40.5 (+5.3)	35.7	37.8 (+2.1)	35.1	36.4 (+1.3)
C	34.7	34.6 (−0.1)	34.2	40.8 (+6.6)	32.5	32.6 (+0.1)	32.5	33.8 (+1.3)	32.1	32.1 (±0.0)
T	37.0	43.7 (+6.7)	37.3	38.1 (+0.8)	32.4	32.4 (±0.0)	32.5	35.5 (+3.0)	33.2	33.9 (+0.7)

[a] Melting temperature was measured as described in the footnote of Figure 3 except for the NaCl concentration in the buffer. **X** represents the base opposite AP.
[b] The buffer contained 100 mM NaCl.
[c] The buffer contained 50 mM NaCl.

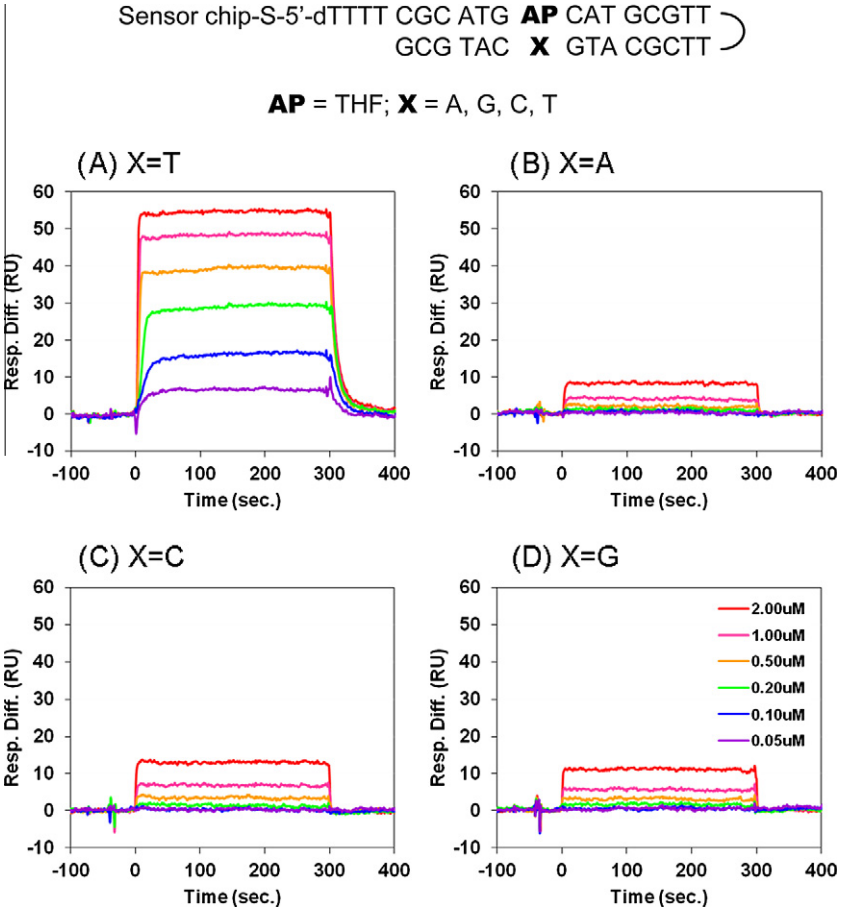

Figure 5. The SPR sensorgrams obtained with A-ligand using a sensor chip immobilizing the hairpin duplex. (A) **X** = T, (B) **X** = A, (C) **X** = C and D) **X** = G. Experiments were performed in 10 mM HEPES–NaOH buffer (pH 7.0) and 100 mM NaCl at 25 °C and the concentration of the A-ligand was from 0.05 to 2.00 μM at the flow rate of 20 μl/min.

T, resulting in an improvement of the selectivity to the opposing A (Fig. 4E, ΔT_m = +4.0 °C). In the control experiments, these ligands did not show any stabilization effect to the full match duplexes lacking the AP site (Table S1). Also 3,3′-diaminodipropylamine, adenine, and cytosine, thymine, or uracil alone did not produce any significant stabilization to the duplex ODN containing the AP site. Guanine was not tested due to its insolubility. These results clearly suggested that the selective stabilization was not exhibited by the polycation, but by the selective interaction of the nucleobase with the nucleobase opposite the AP site pocket.

The increase in the T_m values of the duplex ODN containing the AP site is produced due to the stabilization effect of the ligand not only by the hydrogen bonds and the electrostatic interaction, but also by the stacking interaction of the nucleobase part inserted in the AP site pocket. Therefore, it was assumed that the pyrimidine

Table 2
Equilibrium association constants (K_a, $10^6\ M^{-1}$) of the ligands obtained by the SPR measurements[a]

Ligand	K_a ($\times 10^6\ M^{-1}$)			
	X = A	X = G	X = C	X = T
A-Ligand	0.057	0.087	0.010	3.900
G-Ligand	0.016	0.047	6.300	0.080
C-Ligand	0.002	0.039	0.002	0.001
T-Ligand[b]	0.222	0.043	0.063	0.053
U-Ligand[b]	0.045	0.001	0.022	0.027
norspermidine	—[c]	—[c]	—[c]	<0.001

[a] Equilibrium association constants were obtained from the SPR response by an affinity analysis by steady-state. The measurement was done as described in the footnote of Figure 5.
[b] 50 mM NaCl was used.
[c] Not measured.

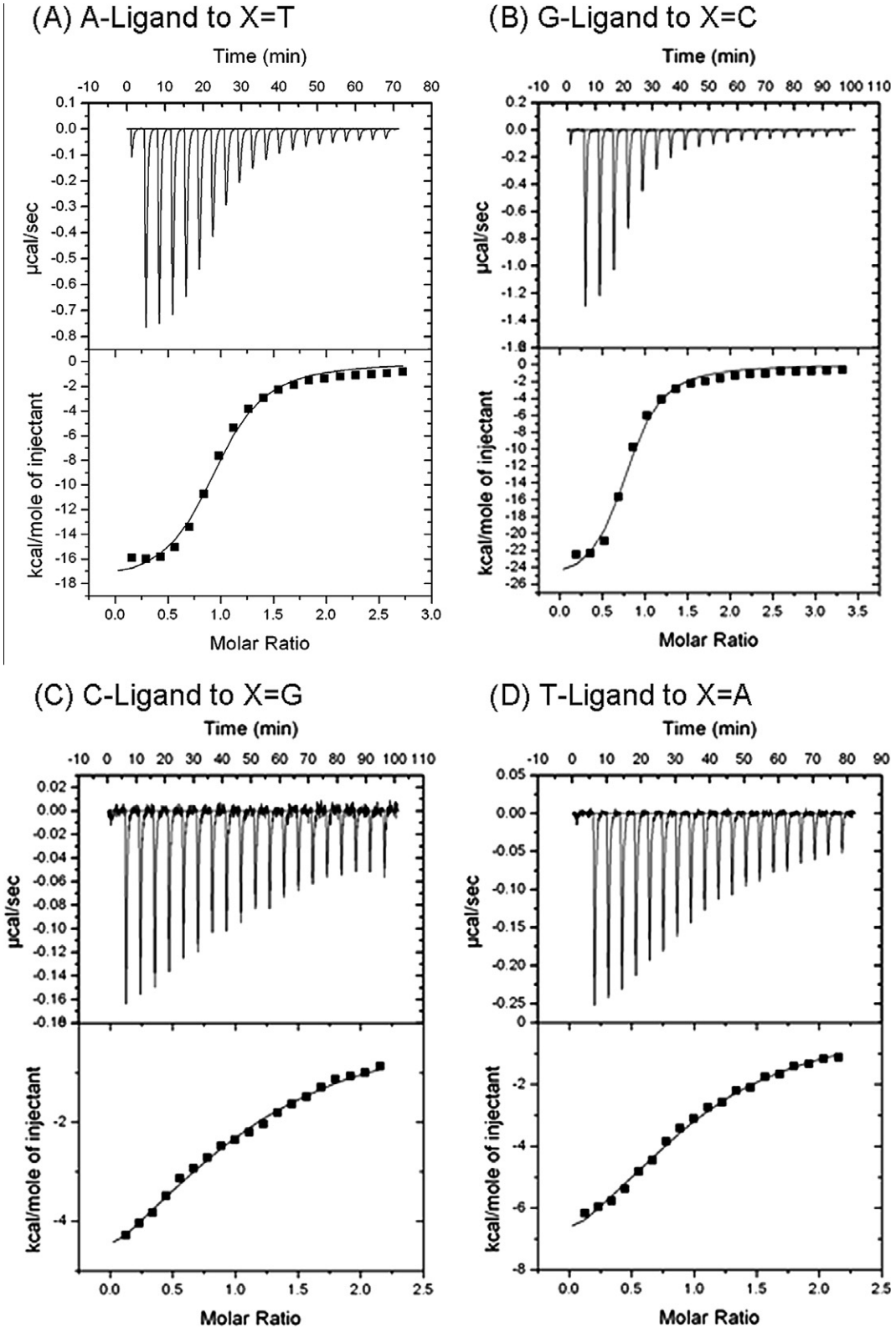

Figure 6. The ITC binding isotherm of the ligand to the selective duplex ODN containing the AP site. Each ligand was added to a solution of the duplex ODN (10 μM, 5′-dGCGTAC **AP** CATGCG-3′/ 5′-dCGCATG **X** GTACGC-3′; **AP** = THF, **X** = A, G, C, T) in 10 mM HEPES–NaOH buffer (pH 7.0) containing 100 mM NaCl at 25 °C. (A) A-ligand to X = T, (B) G-ligand to X = C, (C) C-ligand to X = G, D) T-ligand to X = A.

ligands (C-, T- and U-ligand) would exhibit a lower stacking interaction than the purine ligands (A- and G-ligand) and would produce the lower stabilization effect for the duplex containing the AP site. Thus, the effect of pyrimidine ligands on the T_m values were measured under the lower salt conditions (50 mM NaCl) than those with the purine ligands (100 mM NaCl). Stronger charge interactions were expected to compensate the weaker stacking interactions. The stabilization effect of the T- or U-ligand was

Table 3
The thermodynamic parameters of the binding of the ligand with its selective duplex[a]

Ligand	X	N[b]	ΔH (kcal/mol)	ΔS (kcal/kmol)	$-T\Delta S$ (kcal/mol)	ΔG (kcal/mol)
A-Ligand	T	0.94	−18.17	−32.60	9.72	−8.45
G-Ligand	C	0.87	−26.30	−59.80	17.83	−8.47
C-Ligand	G	1.02	−7.38	−1.07	0.32	−7.06
T-Ligand	A	0.97	−9.56	−7.53	2.25	−7.32
U-Ligand	A	1.04	−3.08	13.50	−4.03	−7.11

[a] The parameters were obtained from the ITC binding isotherm shown in Figures 6 and S6.
[b] Binding stoichiometry.

lower than that of the C-ligand probably because the A-T or A-U base pair is weaker than the G–C base pair. The CD spectrum of the duplex DNA containing the AP site either in the absence or the presence of the ligand showed the typical B-DNA conformation (Fig. S3), suggesting that the duplex DNA conformation was not affected by the binding of the ligand in the AP site pocket.

2.3. Evaluation of the binding affinity of the ligands to the duplex DNA by SPR

We measured the surface plasmon resonance (SPR) to evaluate the binding affinity of the ligand to the duplex DNA containing the AP site. The hairpin duplex DNA having the TTTT loop structure and the AP site (5′-dTTTT CGC ATG **X** GTA CGC TTTT GCG TAC **AP** CAT GCG-3′, **X** = A, G, C, T) labeled with the biotin unit at the 5′ terminus was immobilized onto a streptavidin surface of the sensor chip. The A-ligand produced a sensorgram showing the strong binding to the duplex having the thymidine opposite the AP site (Fig. 5A), but a much lower response was observed for the duplexes having A, G, or C opposite the AP site (Fig. 5B–D).

The polyamine part alone did not produce a significant SPR response, clearly indicating that the selective binding is obtained by the conjugation of the polyamine with the nucleobase part. The selective affinity of the A-ligand to the duplex containing the AP site was well correlated with the increase in the T_m value. Accordingly, the selective interaction of the A-ligand with the duplex DNA containing the AP site has been proved to be responsible for the selective increase of the T_m value. Similarly, the G-, C-, and T-ligands showed the strongest binding to the duplex having the opposing C, G and A, respectively (Fig. S4). Since the T-ligand did not produce a sufficient response for the affinity analysis in the buffer containing 100 mM sodium chloride, the equilibrium association constants were obtained in the presence of 50 mM sodium chloride. The selective combination; that is A-ligand to T, G-ligand to C, C ligand to G, and T-ligand to A, produced the equilibrium association constants ranging from 0.22 to $6.3 \times 10^6\ M^{-1}$, which were 5∼390-fold higher than those for the non-selective combinations (Table 2). In contrast to the UV-melting experiments, the T-ligand exhibited a clear selectivity to the opposing A. In the case of the U-ligand, the A-selectivity observed in the UV-melting experiment was not clear for the SPR measurement.

2.4. Thermodynamic parameters of the binding of the ligand for the duplex containing the AP site

The thermodynamic parameters of the binding of the ligand with the duplex containing the AP site were obtained by isothermal titration calorimetry (ITC). The ligand solution was added to a solution of the duplex and the thermal change was observed. The ITC binding isotherms of the ligands are summarized in Figure 6 and S6, and the obtained parameters are summarized in Table 3. The A-ligand binding to the duplex having the T/AP site was analyzed to produce the 1:1 binding stoichiometry (N = 0.94, Table 3) with a high enthalpy gain and entropy loss (Fig. 7). On the other hand,

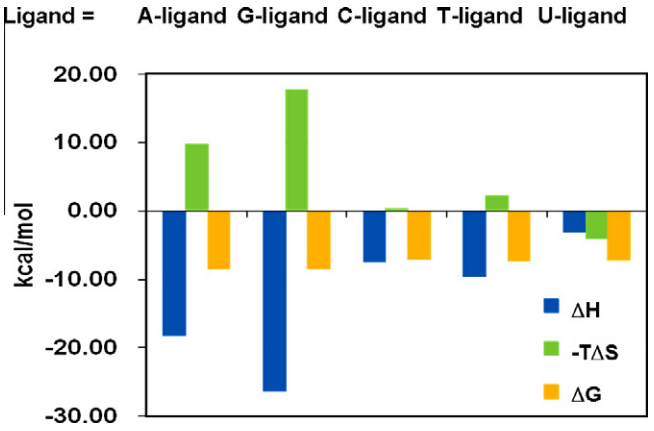

Figure 7. Comparison of thermodynamic parameters summarized in Table 3.

a clear binding isotherm was not obtained for the combination of the A-ligand and the non-selective duplex having the A/AP, G/AP or C/AP site. The single-base loss reduces the free energy of the duplex to the extent of 8–11 kcal/mol and the enthalpy of the duplex to the extent of 29–46 kcal/mol in these sequences.[22] It has been shown that the ligand can compensate for the duplex instability caused by the loss of the single base by binding with the remaining nucleobase in the AP site pocket (the free energy was 7–8 kcal/mol and the enthalpy was 3–33 kcal/mol).

The thermodynamic parameters for the G-ligand binding to X = C were similar to those of the A-ligand in terms of the 1:1 binding stoichiometry, the high enthalpy gain and the entropy loss (Fig. 7). The binding enthalpy must be due to the interactions by hydrogen bonds between the purine base of the ligand and the pyrimidine base opposite the AP site, stacking of the purine base within the flanking cytosine bases, and charge interactions between the polycation part and the phosphate backbone. MD calculations on the duplex having the C/AP or T/AP sites have suggested that the AP site is flexible and adopts a range of conformations.[23] The CD spectra showed a slight change in the B-form conformation of the duplex DNA by binding of the ligand to the AP site (Fig. S3). Therefore, the entropy loss associated with the binding might reflect the decreased flexibility of the local conformation neighboring the AP site.

Interestingly, the binding parameters of the C- and T-ligands were similar to each other and showed a remarkable contrast to those of the A- and G-ligands in that almost no entropy loss is associated with the binding. In the MD calculation on the G/AP site, the α-anomer of the 2′-deoxyribose part adopts an intrahelical conformation, and the guanine is stacked between the flanking bases. The slight entropy loss associated with the binding of the pyrimidine ligands may imply that the conformational change around the AP site is not induced by the binding of the pyrimidine ligand. In the UV-melting experiment, the U-ligand showed a better selectivity to the opposing A than the T-ligand (Fig. 4D vs E). However, the

binding affinity obtained by SPR and also by ITC indicated that the T-ligand has a higher affinity to the adenine opposite the AP site. The thermodynamic parameters of these ligands revealed a sharp contrast, namely, the relatively high enthalpy gain and low entropy loss were observed for the T-ligand, whereas lower enthalpy gain and entropy gain for the U-ligand (Fig. 7). The higher enthalpy gain for the T-ligand may reflect the effects of the methyl group on the hydrogen bonding, stacking interaction, and the hydrophobic interaction.[24] Such interactions also increase the binding affinity for the mismatch base pairs, resulting in low selectivity in the UV-melting experiment (Table 1). The entropy gain observed for the U-ligand binding to the opposing A may be beneficial for keeping the complex during the thermal denaturation in UV-melting experiment. This may account for the fact that a better selectivity to the opposing A was obtained by the U-ligand (Fig. 4E).

3. Conclusion

In this study, we hypothesized the selective formation of Watson–Crick base pairs in the AP site using the nucleobase–polycation conjugates (**1**–**5**). Measurements of the UV-melting showed a high selectivity of A-, G-, C-, and U-ligands for the complementary nucleobases except T-ligand. SPR measurements showed the larger association constants between base-selective conjugates and their complementary nucleobases including C-ligand. And ITC measurements clearly showed that the 1:1 binding stoichiometry between conjugates and their complementary bases. Binding of A- and G-ligands was favored by a high enthalpy gain and entropy loss, suggesting the strong stacking of purine bases. The entropy loss was ascribed to the conformational flexibility from the CD measurements. C- and T-ligands showed almost no entropy loss for the base pairing, and U-ligand showed a lower enthalpy gain compared to T-ligand. In conclusion, this study has clearly demonstrated that the Watson–Crick base pair is generally formed in the AP site pocket using the nucleobase–polyamine conjugates. The new AP site selective ligands may find utility as recognition molecules for the AP site as well as the lead compounds for interference of the AP site associated biological reactions such as polymerization and repair systems.

4. Experimental section

4.1. Method

Melting points were determined using a Stuart Scientific MELTING POINT APPARATUS SMP 3. ^{1}H and ^{31}P NMR spectra were recorded at 400 MHz on a Varian 400 UNITY using $CDCl_3$, CD_3OD, CD_3CN or D_2O as a solvent. ^{13}C NMR spectra were recorded at 125 MHz on a Varian INOVA 500 using D_2O as a solvent. Chemical shifts are reported in ppm, in δ units. ESI-MS spectra were recorded on an Applied Biosystems Marinar System 5299 API-TOF instrument. IR spectra were recorded on a PerkinElmer Spectrum One FT-IR spectrometer.

4.2. 1-*N*-Boc-4-*N*,7-*N*-dinosyl-4-azeheptane-1,7-diamine (6)

A solution of di-*tert*-butyl dicarbonate (9.2 ml, 40.0 mmol) in anhydrous THF (120 ml) was added dropwise over a period of 2.5 h to a solution of 3,3′-diaminodipropylamine (24.3 ml, 172 mmol) in anhydrous THF (180 ml) under an argon atmosphere at 0 °C. This reaction mixture was stirred for 1 day at 0 °C, and then THF was evaporated. The residue was poured into water (100 ml) and the mixture was extracted with CH_2Cl_2 (100 ml × 7). The organic extracts were dried over anhydrous Na_2SO_4, filtered and evaporated to afford a crude product (10.7 g), which was purified by column chromatography (silica gel, CH_2Cl_2/MeOH: 28% aqueous NH_3 = 40:8:1 to 10:4:1) 40:8:1–10:4:1) to give 1-*N*-Boc derivative as a pale yellow oil (8.5 g, 36.7 mmol, 91%).

To a solution of the above 1-*N*-Boc derivative (8.7 g, 37.8 mmol) in anhydrous CH_2Cl_2 (20 ml) were added anhydrous Et_3N (26.3 ml, 189 mmol) and a solution of 2-nitrobenzenesulfonyl chloride (17.6 g, 79.4 mmol) in anhydrous CH_2Cl_2 (40 ml) over a period of 15 min under an argon atmosphere at 0 °C, and the mixture was stirred for 45 min. The reaction mixture was poured into CH_2Cl_2 (150 ml), washed with 1 M aqueous $KHSO_4$ (200 ml), saturated aqueous $NaHCO_3$ (200 ml), and brine (150 ml). The organic extracts were dried over anhydrous Na_2SO_4, filtered and evaporated to afford a crude product (20.9 g), which was purified by column chromatography (silica gel, CH_2Cl_2 to 5% MeOH) to yield **6** as a green foam (17.3 g, 28.7 mmol, 76%). ^{1}H NMR (400 MHz, $CDCl_3$) δ ppm: 8.10–8.08 (1H, m), 7.99–7.97 (1H, m), 7.85–7.83 (1H, m), 7.75–7.67 (4H, m), 7.62–7.60 (1H, m), 5.63 (1H, t, J = 6 Hz), 4.74 (1H, br s), 3.36 (2H, t, J = 7 Hz), 3.31 (2H, t, J = 7 Hz), 3.16–3.09 (4H, m), 1.83 (1H, quint., J = 7 Hz), 1.70 (1H, quint., J = 7 Hz), 1.41 (9H, s). ESI-MS m/z: 602.2 $[M+H]^+$. IR cm^{-1}: 1694, 1542, 1367, 1344, 1164.

4.3. 1-*N*-Boc-7-*N*-(3-bromopropyl)-4-*N*,7-N-dinosyl-4-azeheptane-1,7-diamine (7)

To a solution of **5** (14.6 g, 24.3 mmol) in anhydrous DMF (40 ml) were added K_2CO_3 (16.8 g, 22 mmol) and 1,3-dibromopropane (12.4 ml, 122 mmol) under an argon atmosphere at 0 °C, and the mixture was stirred for 8.5 h at room temperature. The reaction mixture was poured into water (200 ml) and extracted with ether (200 ml × 2). The organic layers were washed with brine (200 ml), dried over anhydrous Na_2SO_4, filtered and evaporated to afford a crude product (20.9 g), which was purified by column chromatography (silica gel, CH_2Cl_2 to 1% MeOH) to yield **7** as a clear yellow viscous oil (12.6 g, 17.4 mmol, 72%). ^{1}H NMR (400 MHz, $CDCl_3$) δ ppm: 8.03–7.97 (2H, m), 7.71–7.66 (4H, m), 7.62–7.59 (2H, m), 3.40 (2H, t, J = 7 Hz), 3.36–3.25 (8H, m), 3.13–3.08 (2H, m), 2.06 (2H, quint., J = 7 Hz), 1.86 (2H, quint., J = 7 Hz), 1.71 (2H, quint., J = 7 Hz), 1.42 (9H, s). ESI-MS m/z: 722.5, 724.5 $[M+H]^+$. IR cm^{-1}: 1705, 1543, 1368, 1346, 1161.

4.4. A-Ligand (1)

A suspension of adenine (393 mg, 2.90 mmol), **7** (1.05 g, 1.45 mmol) and K_2CO_3 (804 mg, 5.81 mmol) in anhydrous DMF (3 ml) was heated under an argon atmosphere at 60 °C for 5.5 days, and then quenched by the addition of water. The reaction mixture was extracted with $CHCl_3$, the organic extracts were washed with brine, dried over anhydrous Na_2SO_4, filtered and evaporated to afford crude products (1.58 g), which was purified by column chromatography (silica gel, $CHCl_3$/MeOH = 20:1) to yield the coupling product **8** as a pale yellow foam (676 mg, 0.87 mmol, 60 %). ^{1}H NMR (400 MHz, $CDCl_3$) δ ppm: 8.29 (1H, s), 7.93 (1H, s), 7.96–7.88 (2H, m), 7.70–7.58 (6H, m), 4.25 (2H, t, J = 7 Hz), 3.33 (2H, t, J = 7 Hz), 3.30–3.22 (6H, m), 3.09 (2H, q, J = 6 Hz), 2.19 (2H, quint., J = 7 Hz), 1.85–1.77 (2H, m), 1.67 (2H, quint., J = 7 Hz),1.41 (9H, s). ESI (MS) m/z: 777.4 $[M+H]^+$. IR cm^{-1}: 1704, 1543, 1367, 1347, 1162.

To a solution of the above coupling product **8** (671 mg, 0.86 mmol) in anhydrous DMF (1.5 ml) were added thiophenol (195 μl, 1.90 mmol) and K_2CO_3 (448 mg, 3.45 mmol) under an argon atmosphere at room temperature. The reaction mixture was stirred for 13 h at room temperature and then quenched by the addition of methanol. This mixture was filtered and the filtrate was evaporated to afford a crude product, which was purified by column chromatography (silica gel, $CHCl_3$/MeOH/aq NH_3 = 20:8:1) to yield the

partially purified products (416 mg). This product was dissolved in 0.5 M HCl/MeOH (26 ml) and the reaction mixture was stirred for 43 h at room temperature, and then the precipitates were collected on a filter, and washed with MeOH to produce **1** as white solids (317 mg). The filtrates were evaporated to give a crude product, which was extracted with water. The water extracts were washed with $CHCl_3$ and freeze-dried to give **1** as white solids (67 mg). The obtained **1** was purified by precipitation from water/EtOH (4 ml/40 ml) at −78 °C. The purified **1** was collected by centrifuged (1500 rpm, 10 min), and dried under vacuum to give **1** as white solids (266 mg, 68% after re-precipitation twice). mp 270–271 °C. ^{1}H NMR (400 MHz, D_2O) δ ppm: 8.36 (1H, s), 8.28 (1H, s), 4.38 (2H, t, J = 7 Hz), 3.13–3.02 (10H, m), 2.28 (2H, quint., J = 7 Hz), 2.10–2.00 (4H, m). ^{13}C NMR (125 MHz, D_2O) δ ppm: 152.9, 151.2, 147.7, 147.1, 120.8, 47.5, 47.3, 47.2, 44.0, 39.2, 28.7, 26.3, 25.3. HR-ESI-MS m/z: 307.2353 $[M+H]^+$ (307.2366 calcd for $C_{14}H_{27}N_8$). IR cm^{-1}: 2954, 2756, 1699, 1595, 1416.

4.5. G-Ligand (2)

A suspension of 2-amino-6-chloropurine (354 mg, 2.09 mmol), **7** (1.00 g, 1.39 mmol) and K_2CO_3 (770 mg, 5.57 mmol) in anhydrous DMF (1.5 ml) was heated under an argon atmosphere at 60 °C for 4.5 days, and then quenched by the addition of water. The reaction mixture was extracted with $CHCl_3$, the organic extracts were washed with brine, dried over anhydrous Na_2SO_4, filtered and evaporated to afford the crude product (1.40 g), which was purified by column chromatography (silica gel, $CHCl_3$ to $CHCl_3$/MeOH = 40:1) to yield the coupling product as a pale yellow foam (536 mg, 0.66 mmol, 47 %). This coupling product (532 mg, 0.66 mmol) was dissolved in 0.5 M HCl/MeOH (19.7 ml) and stirred at 60 °C for 4 days. The solvent was removed by Liebig condenser to yield Boc-deprotected product **9** (511 mg, quant.). ^{1}H NMR (400 MHz, CD_3OD) δ ppm: 9.00 (1H, s), 8.02–7.96 (2H, m), 7.85–7.72 (6H, m), 4.29 (2H, t, J = 7 Hz), 3.45 (2H, t, J = 8 Hz), 3.41 (2H, t, J = 7 Hz), 3.37–3.31 (4H, m), 2.95 (2H, t, J = 8 Hz), 2.24 (2H, quint., J = 7 Hz), 1.96 (2H, quint., J = 7 Hz),1.89 (2H, quint., J = 7 Hz). ESI (MS) m/z: 692.9 $[M+H]^+$. IR cm^{-1}: 1706, 1633, 1604, 1541, 1371, 1343, 1160.

To a solution of the above product **9** (504 mg, 0.66 mmol) in anhydrous DMF (1.5 ml) were added thiophenol (148 μl, 1.44 mmol) and K_2CO_3 (362 mg, 2.62 mmol) under an argon atmosphere at room temperature. The reaction mixture was stirred for 14 h at room temperature and then quenched by the addition of water. The solvent was evaporated to afford the crude product, which was purified by column chromatography (silica gel, $CHCl_3$/MeOH/aqueous NH_3 = 10:5:4) to yield the Ns-deprotected product (517 mg, quant.). This product was dissolved in 0.5 M HCl/MeOH (19.7 ml) and the reaction mixture was stirred for 1 day at room temperature, and then the solvent was removed by Liebig condenser to produce **2** as white solids (347 mg). The obtained **2** was purified by precipitation from water/EtOH (2 ml/40 ml) at −78 °C. The purified **2** was collected by centrifuged (1500 rpm, 10 min), and dried under vacuum to give **2** as white solids (289 mg, 94% after re-precipitation three times). Mp 210–213 °C. ^{1}H NMR (400 MHz, D_2O) δ ppm: 8.08 (1H, s), 4.19 (2H, t, J = 7 Hz), 3.17–3.05 (10H, m), 2.23 (2H, quint., J = 7 Hz), 2.14–2.03 (4H, m). ^{13}C NMR (125 MHz, D_2O) δ ppm: 160.2, 157.0, 153.8, 141.9, 115.9, 47.4, 47.4, 47.3, 47.2, 43.9, 39.3, 28.5, 26.4, 25.3. HR-ESI-MS m/z: 323.2302 $[M+H]^+$ ($C_{14}H_{27}N_8O$ requires 323.2319). IR cm^{-1}: 2959, 2756, 1716, 1644, 1607, 1137, 1108.

4.6. C-Ligand (3)

A suspension of N^4-acetylcytosine (636 mg, 4.15 mmol), **7** (1.30 g, 1.80 mmol) and K_2CO_3 (588 mg, 4.25 mmol) in anhydrous DMF (2.5 ml) was heated under an argon atmosphere at 60 °C for 6 days, and then quenched by the addition of water. The reaction mixture was extracted with $CHCl_3$, the organic extracts were washed with brine, dried over anhydrous Na_2SO_4, filtered and evaporated to afford the crude product (2.22 g), which was purified by column chromatography (silica gel, $CHCl_3$:MeOH = 20:1) to yield the coupling product **10** as a pale yellow foam (806 mg, 1.01 mmol, 56 %). ^{1}H NMR (400 MHz, $CDCl_3$) δ ppm: 7.97–7.93 (2H, m), 7.72–7.66 (4H, m), 7.62–7.56 (2H, m), 7.40 (1H, d, J = 7 Hz), 3.95–3.86 (2H, m), 3.36 (2H, t, J = 7 Hz), 3.32–3.23 (6H, m), 3.16–3.08 (2H, m), 2.07 (2H, quint., J = 7 Hz), 1.88 (2H, quint., J = 7 Hz), 1.42 (9H, s). ESI (MS) m/z: 794.9 $[M+H]^+$. IR cm^{-1}: 1708, 1544, 1370, 1347, 1162.

To a solution of the above coupling product **10** (800 mg, 1.01 mmol) in anhydrous DMF (1.5 ml) were added thiophenol (227 μl, 2.21 mmol) and K_2CO_3 (695 mg, 5.03 mmol) under an argon atmosphere at room temperature. The reaction mixture was stirred for 3.5 h at room temperature and then quenched by the addition of methanol. This mixture was filtered and the filtrate was evaporated to afford a crude product (1.27 g), which was purified by column chromatography (silica gel, $CHCl_3$/MeOH/aqueous NH_3 = 20:8:1–10:4:1) to yield the purified product (399 mg). This product was dissolved in 0.5 M HCl/MeOH (29 ml) and the reaction mixture was stirred for 2 days at room temperature, and then the solvent was removed by Liebig condenser to produce **3** as white solids (362 mg). The obtained **3** was purified by precipitation from water/EtOH (1.5 ml/40 ml) at −78 °C. The purified **3** was collected by centrifuged (1500 rpm, 10 min), and dried under vacuum to give **3** as white solids (291 mg, 67% after re-precipitation twice). Mp 248–249°C. ^{1}H NMR (400 MHz, D_2O) δ ppm: 7.77 (1H, d, J = 8 Hz), 6.12 (1H, d, J = 8 Hz), 3.91 (2H, t, J = 7 Hz), 3.16–3.04 (10H, m), 2.13–2.01 (6H, m). ^{13}C NMR (125 MHz, D_2O) δ ppm: 162.7, 152.6, 151.8, 97.6, 49.4, 47.4, 47.3, 47.2, 47.2, 39.2, 27.6, 26.3, 25.2. HR-ESI-MS m/z: 283.2240 $[M+H]^+$ ($C_{13}H_{27}N_6O$ requires 283.2266). IR cm^{-1}: 2959, 2752, 1707, 1682.

4.7. T-Ligand (4)

A suspension of N^3-benzoylthymine (495 mg, 2.15 mmol), **7** (1.04 g, 1.43 mmol) and K_2CO_3 (792 mg, 5.73 mmol) in anhydrous DMF (1.5 ml) was heated under an argon atmosphere at 60 °C for 6.5 days, and then quenched by the addition of water. The reaction mixture was extracted with $CHCl_3$, the organic extracts were washed with brine, dried over anhydrous Na_2SO_4, filtered and evaporated to afford crude products (1.55 g), which was purified by column chromatography (silica gel, $CHCl_3$/MeOH = 60:1 to 20:1) to yield the coupling product **11** as a pale yellow foam (748 mg, 0.97 mmol, 68 %). ^{1}H NMR (400 MHz, $CDCl_3$) δ ppm: 7.97–7.95 (2H, m), 7.73–7.66 (4H, m), 7.62–7.59 (2H, m), 7.04 (1H, br s), 3.72 (2H, t, J = 7 Hz), 3.36 (2H, t, J = 7.0 Hz), 3.32–3.24 (6H, m), 3.11 (2H, q, J = 6 Hz), 1.97 (4H, quint., J = 7 Hz), 1.90 (3H, s), 1.71 (2H, quint., J = 7 Hz), 1.44 (9H, s). ESI (MS) m/z: 768.1 $[M+H]^+$. IR cm^{-1}: 1684, 1543, 1368, 1347, 1162.

To a solution of the above coupling product **11** (738 mg, 0.96 mmol) in anhydrous DMF (1.5 ml) were added thiophenol (217 μl, 2.11 mmol) and K_2CO_3 (664 mg, 4.80 mmol) under an argon atmosphere at room temperature. The reaction mixture was stirred for 11.5 h at room temperature and then quenched by the addition of methanol. This mixture was filtered and the filtrate was evaporated to afford a crude product (1.71 g), which was purified by column chromatography (silica gel, $CHCl_3$/MeOH = 2:1 to $CHCl_3$:MeOH:aqueous NH_3 = 20:8:1) to yield the purified product (376 mg). This product was dissolved in 0.5 M HCl/MeOH (28 ml) and the reaction mixture was stirred for 1 day at room temperature, and then the solvent was removed by Liebig condenser to produce **4** as white solids (361 mg). The obtained **4** was purified by reprecipitation from water/EtOH (3 ml/40 ml) at −78 °C. The

purified **4** was collected by centrifuged (1500 rpm, 10 min), and dried under vacuum to give **4** as white solids (276 mg, 70% after precipitation twice). Mp 243–244 °C. ^{1}H NMR (400 MHz, D_2O) δ ppm: 7.42 (1H, s), 3.81 (2H, t, J = 7 Hz), 3.14–3.03 (10H, m), 2.10–2.00 (6H, m), 1.82 (3H, s). ^{13}C NMR (125 MHz, D_2O) δ ppm: 169.5, 155.1, 145.2, 113.9, 48.0, 47.4, 47.3, 47.2, 47.1, 39.2, 27.8, 26.3, 25.2, 13.9. HR-ESI-MS *m/z*: 298.2237 $[M+H]^+$ ($C_{14}H_{28}N_5O_2$ requires 298.2266). IR cm^{-1}: 2952, 2756, 1699, 1664.

4.8. U-Ligand (5)

A suspension of N^3-benzoyluracil (448 mg, 2.07 mmol), **7** (1.02 g, 1.41 mmol) and K_2CO_3 (763 mg, 5.52 mmol) in anhydrous DMF (5 ml) was heated under an argon atmosphere at 80 °C for 4 days, and then quenched by the addition of water. The reaction mixture was extracted with $CHCl_3$, the organic extracts were washed with brine, dried over anhydrous Na_2SO_4, filtered and evaporated to afford crude products (1.75 g), which was purified by column chromatography (silica gel, $CHCl_3$/MeOH = 100:1 to 40:1) to yield the coupling product **12** as a pale yellow foam (769 mg, 1.02 mmol, 72 %). ^{1}H NMR (400 MHz, CD_3CN) δ ppm: 7.91–7.88 (2H, m), 7.79–7.70 (6H, m), 7.29 (1H, d, J = 8 Hz), 5.53 (1H, d, J = 8 Hz), 3.64 (2H, t, J = 7 Hz), 3.31–3.22 (8H, m), 2.80 (2H, q, J = 6 Hz), 1.85 (4H, m), 1.67–1.60 (2H, m), 1.39 (9H, s). ESI (MS) *m/z*: 754.1 $[M+H]^+$. IR cm^{-1}: 1682, 1543, 1369, 1346, 1162.

To a solution of the above coupling product **12** (240 mg, 0.32 mmol) in anhydrous DMF (700 µl) were added thiophenol (70 µl, 0.70 mmol) and K_2CO_3 (177 mg, 1.28 mmol) under an argon atmosphere at room temperature. The reaction mixture was stirred for 4 h at room temperature and then quenched by the addition of methanol. This mixture was filtered and the filtrate was evaporated to afford a crude product (523 mg), which was purified by column chromatography (silica gel, $CHCl_3$/MeOH/aqueous NH_3 = 40:8:1) to yield the purified products (128 mg). This product (140 mg) was dissolved in 0.5 M HCl/MeOH (1 ml) and the reaction mixture was stirred for 3 days at room temperature, and then the solvent was removed by Liebig condenser to produce **5** as white solids (72.7 mg, 58%). Mp 260–261° C. ^{1}H NMR (400 MHz, D_2O) δ ppm: 7.59 (1H, d, J = 8 Hz), 5.79 (1H, d, J = 8 Hz), 3.85 (2H, t, J = 7 Hz), 3.16–3.04 (10H, m), 2.12–2.01 (6H, m). ^{13}C NMR (125 MHz, D_2O) δ ppm: 169.3, 155.1, 149.5, 104.6, 48.3, 47.4, 47.3, 47.2, 47.1, 39.1, 27.7, 26.3, 25.2. HR-ESI-MS *m/z*: 284.2077 $[M+H]^+$ (284.2081 calcd for $C_{13}H_{26}N_5O_2$). IR cm^{-1}: 3405, 1544, 1368, 1164.

4.9. Synthesis of ODN containing the AP site analogue and complementary ODN

All oligonucleotides were synthesized using solid phase phosphoroamidite chemistry on a Applied Biosystems 394 DNA/RNA synthesizer or a NIHON TECHNO SERVICE H-Series synthesizer. The cleaved oligonucleotides were purified by HPLC on a Waters X-Bridge C18 column using a linear gradient between the 0.1 M TEAA buffer and CH_3CN. The MALDI-TOF/MS was measured on a BRUKER DALTONICS microflex-KS spectrometer and these data were summarized in Supplementary data. Oligonucleotide concentrations were determined spectrophotometrically by measuring the absorbance at 260 nm.

4.10. Evaluation of the stability of duplex ODNs containing the AP site by thermal denaturation studies

All duplexes melting curves were measured on a UV BECKMAN COULTER DU800 in the absence and presence of 20 µM ligand, at a concentration of 4 µM duplex in 10 mM HEPES–NaOH buffer (pH 7.0) at a heat rate of 1 °C/min (from 20 to 80 °C) and a scan rate of 1 °C/min. As a pretreatment, all samples are heated for 5 min at 80 °C and then gradually cooled down. Obtained melting curves were analyzed by non-linear fitting and each melting temperature was determined. $\Delta T_m = T_m(+) - T_m(-)$.

4.11. Evaluation of binding affinities of ligands and hairpin loop duplex ODNs by SPR

All samples were measured on a BIACORE3000. The immobilization of hairpin loop ODNs (Biothin-5′-d TTTT CGC ATG X GTA CGC TTTT GCG TAC **AP** CAT GCG-3', **X** = A, G, C, T) were performed in HBS–N buffer (10 mM HEPES buffer (pH 7.4), 150 mM NaCl) with flow rate of 10 µl/min at 25 °C. The sensorgrams for the interaction of each ligand with 5′-biotin-labeled ODNs were collected in 10 mM HEPES–NaOH buffer (pH 7.0), 100 mM NaCl for A-, G-ligands, 50 mM NaCl for C-, T-, or U-ligands at 25 °C. Each ligand concentrations were from 0.05 to 2.00 µM and ligand solutions were injected 100 µl at a flow rate of 20 µl/min over a period of 300 sec and were followed by 120 s dissociation time. Obtained data were fitted with a one-site model to calculate an equilibrium binding constant.

4.12. Thermodynamics of ligands against complementary duplex ODNs containing the AP site by ITC

All samples were measured on a MicroCal VP-ITC microcalorimeter. 10 µM duplex ODN solutions (1.43 ml) were titrated with 150 µM ligand solutions 19 times, 10 µl per injection except for first injection. The first injection volume was 2 µl and this data was excluded from analysis. Obtained data were fitted with a one-site model to calculate the thermodynamic parameters.

Acknowledgements

This work was supported by a Grant-in-Aid for Scientific Research (S) from the Japan Society for Promotion Science (JSPS) and CREST from the Japan Science and Technology Agency. Y.A. is grateful for the financial support by the Sasagawa Scientific Research Grant from the Japan Science Society.

Supplementary data

Supplementary data associated with this article can be found, in the online version, at http://dx.doi.org/10.1016/j.bmc.2012.04.009.

References and notes

1. Barnett, R. N.; Cleveland, C. L.; Landman, U. *Acc. Chem. Res.* **2010**, *43*, 280.
2. Drabløs, F.; Feyzi, E.; Aas, P. A.; Vaagbø, C. B.; Kavli, B.; Bratlie, M. S.; Peña-Diaz, J.; Otterlei, M.; Slupphaug, G.; Krokan, H. E. *DNA Repair* **2004**, *3*, 1389.
3. (a) Zang, H.; Cates, K. S. *Chem. Res. Toxicol.* **2003**, *16*, 1539; (b) Viswesh, V.; Gates, K.; Sun, D. *Chem. Res. Toxicol.* **2010**, *23*, 99.
4. (a) Fronza, G.; Gold, B. *J. Cell. Biochem.* **2004**, *91*, 250; (b) Connor, E. E.; Wilson, J. J.; Wyatt, M. D. *Chem. Res. Toxicol.* **2005**, *18*, 87.
5. Friedman, J. I.; Stivers, J. T. *Biochemistry* **2010**, *49*, 4957.
6. Lindahl, T.; Nyberg, B. *Biochemistry* **1972**, *11*, 3610.
7. (a) Zerbe, L. K.; Goodman, M. F.; Efrati, E.; Kuchta, R. D. *Biochemistry* **1999**, *38*, 12908; (b) Maga, G.; van Loon, B.; Crespan, E.; Villani, G.; Hübscher, U. *J. Biol. Chem.* **2009**, *284*, 14267.
8. (a) Sagher, D.; Strauss, B. *Biochemistry* **1983**, *22*, 4518; (b) Kunkel, T. A. *Proc. Natl. Acad. Sci. U.S.A.* **1984**, *81*, 1494; (c) Obeid, S.; Blatter, N.; Kranaster, R.; Schnur, A.; Diederichs, K.; Welte, W.; Marx, A. *EMBO J.* **2010**, *29*, 1738.
9. (a) Kingma, P. S.; Osheroff, N. *J. Biol. Chem.* **1997**, *272*, 1148; (b) Kingma, P. S.; Greider, C. A.; Osheroff, N. *Biochemistry* **1997**, *36*, 5934.
10. Dahlmann, H. A.; Vaidyanathan, V. G.; Sturla, S. J. *Biochemistry* **2009**, *48*, 9347.
11. Liu, L.; Yan, L.; Donze, J. R.; Gerson, S. L. *Mol. Cancer Ther.* **2007**, 1061.
12. Belmont, P.; Jourdan, M.; Demeunynck, M.; Constant, J.-F.; Garcia, J.; Lhomme, J. *J. Med. Chem.* **1999**, *42*, 5153.
13. Dhar, S.; Kodama, T.; Greenberg, M. M. *J. Am. Chem. Soc.* **2007**, *129*, 8702.
14. Reco, N. J.; Tor, Y. *J. Am. Chem. Soc.* **2005**, *127*, 10784.
15. Oshimoto, K.; Nishizawa, S.; Minagawa, M.; Teramae, N. *J. Am. Chem. Soc.* **2003**, *125*, 8982.

16. Berthet, N.; Boudali, A.; Constant, J. F.; Decout, J. L.; Demeunynck, M.; Fkyerat, A.; Garcia, J.; Laayoun, A.; Michon, P.; Lhomme, J. *J. Mol. Recognit.* **1994**, *7*, 99.
17. Lhomme, J.; Constant, J. F.; Demeunynck, M. *Biopolymers* **1999**, *52*, 65.
18. Yamamoto, S.; Shinoda, S.; Makita, M. *Biochem. Biophys. Res. Commun.* **1979**, *87*, 1102.
19. (a) Hirschman, S. Z.; Leng, M.; Felsenfeld, G. *Biopolymers* **1967**, *5*, 227; (b) Tabor, H. *Biochemistry* **1962**, *1*, 496.
20. Patel, M. M.; Anchordoquy, T. *J. Biophys. Chem.* **2006**, *122*, 5.
21. Labadi, I.; Jenei, E.; Lahti, R.; Lönnberg, H. *Acta Chem. Scand.* **1991**, *45*, 1055.
22. Gelfand, C. A.; Plum, G. E.; Grollman, A. P.; Johnson, F.; Breslauer, K. J. *Biochemistry* **1998**, *37*, 7321.
23. Chen, J.; Dupradeau, F.-Y.; Case, D. a.; Turner, C. J.; Stubbe, J. *Nucleic Acids Res.* **2008**, *36*, 253.
24. Šponer, J.; Leszczynski, J.; Hobza, P. *Biopolymers* **2002**, *61*, 3.